Radiocarbon, Vol 66, Nr 5, 2024, p 1248–1258 DOI:10.1017/RDC.2023.105
Selected Papers from the 24th Radiocarbon and 10th Radiocarbon & Archaeology International Conferences, Zurich, Switzerland, 11–16 Sept. 2022

HOLOCENE OVERWASH OCCURRENCE AGE IN THE ISUMI RIVER LOWLAND, EASTERN BOSO PENINSULA, JAPAN

Soichiro Oda[1] • Stephen P Obrochta[1]* • Osamu Fujiwara[2] • Yusuke Yokoyama[3] • Yosuke Miyairi[3] • Yoshiya Hatakeyama[1]

[1]Graduate School of International Resource Science, Akita University, 1-1 Tegata Gakuen-machi, Akita 010-8502, Japan
[2]Geological Survey of Japan, National Institute of Advanced Industrial Science and Technology, AIST Central 7, 1-1-1 Higashi, Tsukuba, Ibaraki 305-8567, Japan
[3]Atmosphere and Ocean Research Institute, Tokyo University, 5-1-5, Kashiwanoha, Kashiwa-shi, Chiba 277-8564, Japan

ABSTRACT. Analysis of the chronological data and observation of a lagoonal sediment core reveal sand washover events between around 2.4 to 2.5 cal. ky BP in the Isumi River lowland. We conducted radiocarbon dating with AMS and constructed an age-depth model using the latest calibration curve and appropriate model routine. In the middle to lower part of the core, dark-gray sand layers are repeatedly deposited. Sand layers may exhibit an erosional surface at the base with fining upward grading. The overwash layers are composed of well-rounded sand with occasional gravel, indicative of transportation. overwash sediment characteristics are consistent with proximal marine deposits, suggesting an ocean origin (though riverine sediment is also similar in character). The age-depth model indicates very high sediment accumulation rates associated with overwash deposits. Based on the amount of accumulated sediment, relatively large-scale redeposition events occurred during this period but more information is needed to constrain the mechanism(s) causing the events. We also present a local reservoir age correction compatible with the Marine20 calibration curve.

KEYWORDS: age depth model, overwash, radiocarbon AMS dating.

INTRODUCTION

The purpose of this study is to create an age-depth model using the sediment core collected from the Isumi River lowland and to confirm overwash layers. Radiocarbon dating was performed on both terrestrial plant samples and bulk samples, allowing discussion of the age offsets. In the Boso Peninsula, overwash may be caused by a variety of factors. This area was originally a drowned valley formed during the post-glacial transgression, and subsequent sedimentation and uplift have turned it into an estuarine lowland (Sakai et al. 2006). The bay was closed off from the open ocean due to the development of a barrier system and sediment transported by the longshore current infilled the bay.

The Boso Peninsula is a tectonically active area on the Pacific coast of central Japan where three plates converge offshore to the southeast. These are the North American Plate, the Eurasian Plate, and the Philippine Sea Plate that form a triple junction. The associated ocean trenches are the Japan Trench, Sagami Trough, Izu-Bonin Trench, and Nankai Trough. On the Pacific Ocean side, river and coastal terraces have developed due to past seismic uplift. The tectonic activity promoted valley-fill sedimentation in the area. Barrier development and valley-fill reduced the influence of seawater, creating an environment where mud and/or silt are slowly deposited. Such an environment is suitable for the study of the overwash deposit, which primarily consists of sand because the deposits may be readily differentiated.

STUDY AREA

The Isumi River lowland is in the eastern part of the Boso Peninsula (Figure 1) and extends approximately 6 km from north to south and 2 km from east to west. The maximum tidal range along the Pacific coast of Boso is 1.0 m. The Isumi River is 67.5 km long and has an about

*Corresponding author. Email: obrochta@gipc.akita-u.ac.jp

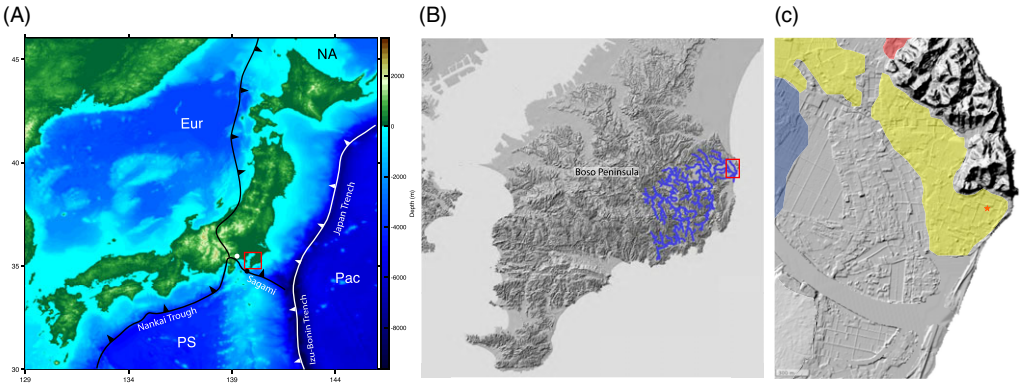

Figure 1 (A) Map of Japan using etopo1 elevation data: White and black circles respectively show the approximate location of the epicenters of the 1923 Taisho and 1703 Genroku Earthquakes. Box shows the area in panel B. (B) Shaded terrain map of the Boso Peninsula. Box shows the area in Panel C. Isumi River drainage extent is shown in blue. (C) Isumi region and the on-land location of Core ISL-6 (star) with the Izumi (dunes), Choja (lagoon), and Fukuhara Surfaces shaded in white, red, and blue, respectively (Nagasawa 1979; note that the Izumi lagoon and Choja dune surface exist but are not in range of Panel C.). Shaded terrain data from the Geospatial Information Authority of Japan (https://www.gsi.go.jp/bousaichiri/hillshademap.html). River data is from the National Land Information Division of the Ministry of Land, Infrastructure, Transport and Tourism (https://geoshape.ex.nii.ac.jp/river/resource/120010/). (Please see online version for color figures.)

300 km^2 drainage area (the largest river of those discharging on the Pacific Ocean side of the Boso Peninsula) and flows east to west through the middle of the lowland to the Pacific Ocean. Terrace developments are recognized in the Isumi River lowland (Nagasawa 1979; Sakai et al 2006; Utsunomiya and Oi 2019). Three major terraces in the area are the Choja, Izumi, and Fukuhara surfaces. Our study area is located in the northeastern part of the Isumi River and is blocked on the seaward side by dunes and is on the Izumi Surface.

Isumi River lowland was formed by sediment transport by the longshore current. The depositional process and landforms from about 11.0 cal. ky BP to 3.0 cal. ky BP are reconstructed from valley-fill deposits affected by rapid tectonic uplifts (Sakai et al. 2006). The sediment progradation occurred during a period of rapid sea level rise between 9.0 to 8.5 cal. ky BP. This was due to an increase in sediment supply caused by tectonic uplift associated with a large earthquake. The Paleo-Isumi Bay extended inland around 7.0 cal. ky BP due to postglacial marine transgression. The Choja and Izumi surfaces formed sometime after 6.5 cal. ky BP and around 3.5 cal. ky BP, respectively, and the modern barrier formed about the same time as the Izumi Surface emergence. The barrier enclosed the remnant Paleo-Isumi Bay, forming a small lagoon. The lagoon was filled by the progradation of small delta and by sediments deposited by large waves from the outside of the barrier. The study area's proximity to the Ocean and large river makes it prone to overwash due to flood and wind waves.

MATERIALS AND METHODS

Sample and Description of the ISL-6

We analyzed a 3.3 m long sediment boring core, ISL-6, recovered from the former lagoon on the northeastern part of the Isumi River lowland, approximately 150 m inland from the modern coastline. The core was collected during a research observation conducted by the National Institute of Advanced Industrial Science and Technology (AIST; Shishikura et al. 2013).

https://doi.org/10.1017/RDC.2023.105 Published online by Cambridge University Press

While the core was photographed in the field, the image resolution was relatively low. We therefore re-imaged it using a portable core scanner known as *The Namahage*, which is a portable core imaging device that produces continuous images, similar to a traditional "line scanner" by using computer vision techniques to create a low distortion composite image from photographs taken at an approximate 5-cm interval. It has been successfully used previously in lacustrine environments (Obrochta et al. 2018). We also obtained CT images of the core at AIST that allow us to examine the internal structure and estimate sediment density. Relatively dense sand beds have a higher CT value, while less dense mud beds have lower CT values. The use of CT images allows more precise identification of overwash deposits. Finally, we conducted CNS elemental analysis using an elemental analyzer (Vario MACRO cube) at AORI (Atmosphere and Ocean Research Institute of Tokyo University).

Age-Depth Model

Radiocarbon dating was conducted on 5 terrestrial plant samples and 11 bulk samples using accelerator mass spectrometry (AMS) at AORI (Atmosphere and Ocean Research Institute of Tokyo University). Three plant fragments were sent to paleo labo for dating shortly after core recovery but have not yet been published and are included here. Bulk samples were selected with high carbon content based on elemental analysis data. Bulk samples were also taken from directly above and below the overwash layers. We used automatic graphitization at AORI that can perform graphitization by simply inserting samples to the elemental analyzer (e.g., Yokoyama et al. 2022). Obtained determinations were calibrated to calendar years by using MatCal (Lougheed and Obrochta 2016) using IntCal20 (Reimer et al. 2020). We used *Undatable* (Lougheed and Obrochta 2019) for age-depth modeling, which is a very fast, frequentist, age model routine. The reader is referred to Lougheed and Obrochta (2019) and to Nara-Watanabe et al. (2023) for more detailed descriptions and comparison with Bayesian methods. It includes both depth and age uncertainty. A certain percentage of data can be bootstrapped out of each simulation, which is useful when not all determinations are in stratigraphic order. If radiocarbon determinations were performed on different material, those materials can be weighted differently by selectively not bootstrapping higher-quality material, giving for example terrestrial material priority over bulk organic matter.

The following is a summary of age-depth model conditions in this study. Bootstrapping was not performed on leaf samples, which are more reliable than bulk samples.

Conditions of Age-Depth Model

Software: Undatable (Lougheed and Obrochta 2019)

1. Four plant fragments from 270 to 273 cm treated as replicate samples.
2. Bulk determinations: 11 (corrected for offset from plant fragments; see below)
3. Plant fragment determinations: 8
4. 100,000 iteration Monte Carlo simulation
5. 30% bootstrapping of bulk dates (no bootstrapping of leaves)
6. Sedimentation date uncertainty factor 0.1
7. IntCal20 (Reimer et al. 2020) for calibration

Bulk ages are systematically older than the plant fragments. The offset between the plant fragments and bulk dates was assessed by using *Undatable* to separately model the median radiocarbon age of both types of material (Figure 2a). The above parameters were used for modeling. The median modeled radiocarbon age of the plant fragments was then subtracted

https://doi.org/10.1017/RDC.2023.105 Published online by Cambridge University Press

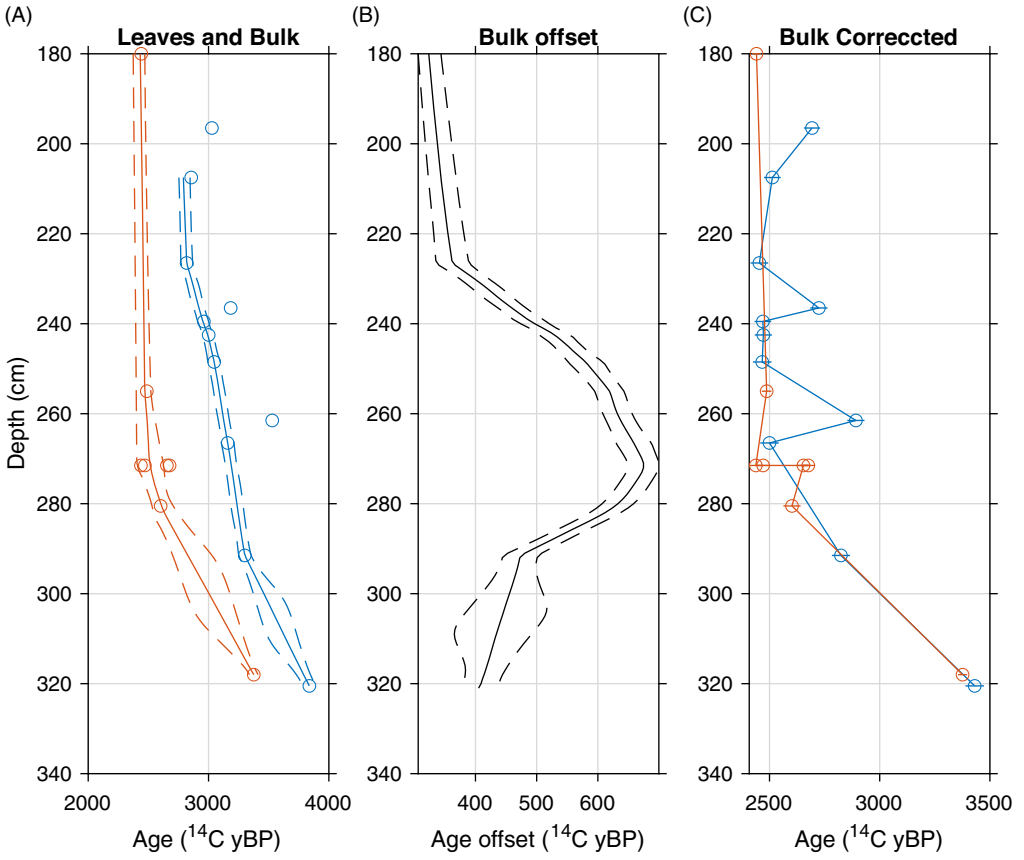

Figure 2 Bulk organic matter age offset: (A) Median model radiocarbon age and 1σ range for plant fragments (red) and bulk organic matter (blue). (B) Age difference (solid line) and 1σ between plant fragments and bulk organic matter. (C) Plant fragment radiocarbon dates (red) plotted with bulk dates (blue) after subtraction of offset. Horizontal lines indicate 1σ uncertainty for use in age modeling.

from the bulk median. This offset (Figure 2b, solid line) was subtracted from each bulk radiocarbon age prior to age modeling (Figure 2c). The analytical uncertainty of the bulk dates was increased based on the modeled 1 σ range (Figure 2b, dashed lines) using root mean sum of squares.

Updated Marine Reservoir Age

Though C/N ratios indicate organic matter is primarily terrestrial in origin (See Results), we also re-calculated the local reservoir value (ΔR) to be compatible with the Marine20 calibration curve. This will be of use for future researchers. Uplift during two historical earthquakes, the 1932 CE Taisho and the 1703 CE Genroku subaerially exposed seafloor, creating terraces on the Miura Peninsula. Shishikura et al. (2007) performed radiocarbon dating on shells sampled from the uplifted terraces, obtaining ΔR of 82 ± 33 and 77 ± 32 for the Taisho and Genroku Earthquakes, respectively for the Marine04 calibration curve. We applied the same method as Shishikura et al. (2007) to obtain ΔR relative to Marine20. Uncertainty in ΔR is calculated by root sum of squares.

https://doi.org/10.1017/RDC.2023.105 Published online by Cambridge University Press

RESULTS

Dating Results

Radiocarbon dating results are shown in Table 1, corrected age and each offset are shown in Table 2. The range is about 2400 to 4000 ^{14}C y BP. Calibrated ages range from 2.4 to 3.5 cal. ky BP. Samples generally show stratigraphically consistent ages (Figure 3), but bulk ages tend to be older than plant ages. In the model, a rapid sediment supply occurs around 2.5 cal. ky BP in the 1.8 to 2.7 m as evidenced by reliable plant sample ages. The data density is relatively high in this range, and the probability density is approximately within error. The sediment accumulation rate (SAR) in the deeper portion of the core is less than 5 cm/ky, but the maximum sedimentation rate around 2.5 cal. ky BP is over 1100 cm/ky, indicating rapid sedimentation supply.

Sediment Description

The upper part of the core, from 0 to 1.2 m is reclaimed landfill. A muddy silt is deposited below this from 1.2 to 3.2 m, overlying a peat deposit. The muddy silt interval typically exhibits C/N values of ~15 or higher, though with some lower values. The typical C/S value for the muddy silt is ~2–3. Dark-gray sand layers are repeatedly deposited below ~1.7 m (Figure 4).

Event Deposits

We identified up to nine sandy event layers. The sand grains are composed of well-rounded sand with occasional rounded gravel that are most likely derived from the beach based on the characteristics of the grains and facies. The layers are composed of a single layer or multiple, thin alternating layers, some of which have erosional surface at the base and exhibit fining upward grading. The multiple layers contain fine alternating sand and silt layers. The maximum event layer thickness is 30 cm, and the minimum is 3 cm. In the lower part of the core, there is an abrupt change in facies from light-colored muddy silt layers to peat layers.

Marine20 Local Reservoir Correction

We obtained ΔR values of –69 ± 76 and –113 ± 81 years for the from the 1923 CE Taisho and 1703 CE Genroku uplifted terraces, respectively (Table 3). The built-in Marine20 reservoir age is generally ~150 years older than previous calibrations curves. Thus, previously positive local corrections become negative. We recommend use of the average ΔR, which is is –91 ± 111 years.

DISCUSSION

We identified the nine sand layers that were repeatedly deposited in an otherwise low-energy, back-barrier muddy lagoon environment. The relatively high C/N ratio suggest organic matter is primarily terrigenous, though with some mixing of aquatic organic matter because C/N ratios of freshly deposited organic matter derived mainly from plankton range between 6 and 9 (Biggs et al. 1983) while terrestrial plants are generally above 15 (Orem et al. 1991).

Variations in C/S ratio likely reflect changes in redox state caused by washover events breaching the barrier. A C/S ratio above five is indicative of freshwater, while values near three are typical of fine seafloor sediment deposited in an oxic environment. Values near one are commonly exhibited by sediment deposited in poorly oxygenated bays and estuaries

https://doi.org/10.1017/RDC.2023.105 Published online by Cambridge University Press

Table 1 Radiocarbon dating result. The radiocarbon ages are from 8 plant fragments, 11 bulk samples.

#	Lab code	Center depth (cm)	Material	^{14}C age (yr)	^{14}C error (yr)	2 sigma range (yr)
1	PLD-23279; leaf	180	Terrestrial plant	2441	20	2360–2696
2	YAUT-068931; Isumi-93; bulk	196.5	Sediment (bulk)	3028	30	3082–3345
3	YAUT-068929; Isumi-87; bulk	207.5	Sediment (bulk)	2856	30	2875–3068
4	YAUT-068928; Isumi-68; bulk	226.5	Sediment (bulk)	2818	29	2848–3052
5	YAUT-068926; Isumi-58; bulk	236.5	Sediment (bulk)	3184	31	3358–3455
6	YAUT-068925; Isumi-55; bulk	239.5	Sediment (bulk)	2961	30	3003–3213
7	YAUT-068924; Isumi-52; bulk	242.5	Sediment (bulk)	3001	30	3074–3330
8	YAUT-068923; Isumi-46; bulk	248.5	Sediment (bulk)	3047	31	3170–3353
9	PLD-23280; leaf	255	Terrestrial plant	2487	22	2471–2719
10	YAUT-068919; Isumi-35; bulk	261.5	Sediment (bulk)	3529	31	3699–3893
11	YAUT-068918; Isumi-30; bulk	266.5	Sediment (bulk)	3159	31	3271–3450
12	YAUT-068933; Isumi_70.5-71; leaf	270.5	Terrestrial plant	2438	30	2357–2699
13	YAUT-068936; Isumi_71-72; leaf	271.5	Terrestrial plant	2471	29	2372–2715
14	YAUT-068937; Isumi_72-73; leaf	272.5	Terrestrial plant	2676	31	2747–2847
15	YAUT-071628; Isumi_72-73; leaf	272.5	Terrestrial plant	2654	32	2736–2847
16	YAUT-069526; Isumi-77-84; leaf	280.5	Terrestrial plant	2602	39	2520–2839
19	YAUT-068915; Isumi-5; bulk	291.5	Sediment (bulk)	3301	30	3451–3577
20	PLD-23284; leaf	318	Terrestrial plant	3376	21	3520–3690
21	YAUT-068932; Isumi-115; bulk	320.5	Sediment (bulk)	3838	31	4104–4404
	Depth range	180–330	**^{14}C age range**	2400–4000		

Table 2 Corrected bulk radiocarbon ages and each offset from plant fragment ages (Figure 2B). Errors are instrumental error reported in Table 1 combined with the uncertainty in Figure 2B using root mean sum of squares. Total organic carbon is also reported as it was the basis for bulk sample selection, as is molar C/N and C/S ratios.

Lab code	Center depth	Uncorrected ^{14}C age (yr)	Corrected ^{14}C age (yr)	Corrected ^{14}C error (yr)	Offset (yr)	Carbon content (%)	C/N ratio	C/S ratio
YAUT-068931; Isumi-93; bulk	196.5	3028	2693	37	335	3.08	21.05	8.5
YAUT-068929; Isumi-87; bulk	207.5	2856	2513	38	343	2.45	21.67	5.66
YAUT-068928; Isumi-68; bulk	226.5	2818	2454	40	364	5.55	25.75	6.59
YAUT-068926; Isumi-58; bulk	236.5	3184	2724	39	460	3.42	20.69	3.84
YAUT-068925; Isumi-55; bulk	239.5	2961	2470	38	491	3.83	21.65	4.67
YAUT-068924; Isumi-52; bulk	242.5	3001	2472	39	529	4.30	26.6	4.32
YAUT-068923; Isumi-46; bulk	248.5	3047	2467	42	580	3.08	19.1	5.63
YAUT-068919; Isumi-35; bulk	261.5	3529	2892	39	637	2.80	20.74	3.87
YAUT-068918; Isumi-30; bulk	266.5	3159	2500	42	659	2.80	19.41	3.42
YAUT-068915; Isumi-5; bulk	291.5	3301	2824	41	477	2.32	19.2	3.01
YAUT-068932; Isumi-115; bulk	320.5	3838	3431	42	407	4.96	15.89	2.45

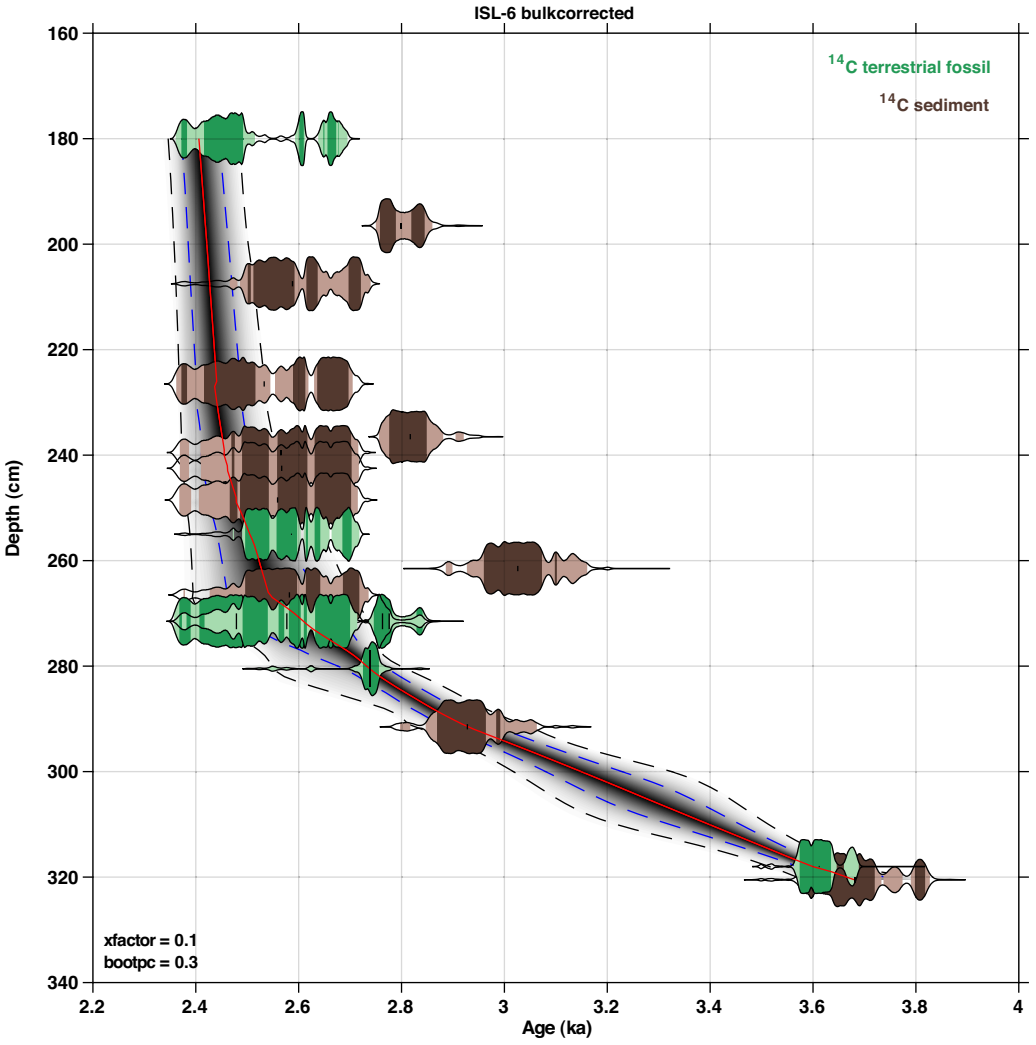

Figure 3 Age-depth model. ISL-6 age model based on the IntCal20 (Reimer et al. 2020) calibration curve. The red line is the median age produced by the model routine Undatable (Lougheed and Obrochta 2019). Dashed blue and black lines are the 1σ and 2σ ranges. Shading represents the 1st to 99th percentiles (darkest is the 50th percentile). Calibrated radiocarbon dates are shown as probability density functions (PDFs). Green are plant fragments and brown are bulk ages after correction for offset from plant fragments. Dark shading denotes the calibrated 1σ intervals, while light shading indicates the 2σ region.

(Berner and Raiswell 1984; Sampei et al. 1997). The transition from peat to silt deposits is consistent with increasing relative sea level in the lower part of the core. Overall, sulfur exhibits a decreasing upward trend, suggesting a diminishing marine influence over time. This could be caused by both lowered sea level, uplift, or an increasingly well-developed coastal barrier. While regional uplift is documented at ~3.5 ka (Sakai et al. 2006), the event layers identified here were deposited ~1000 years later and thus not correlatable to any known uplift events.

The age-depth model indicates that sedimentation occurred rapidly, particularly between 1.8 m and 2.7 m, where the sand layers are concentrated. No significant sand layer is detected above

https://doi.org/10.1017/RDC.2023.105 Published online by Cambridge University Press

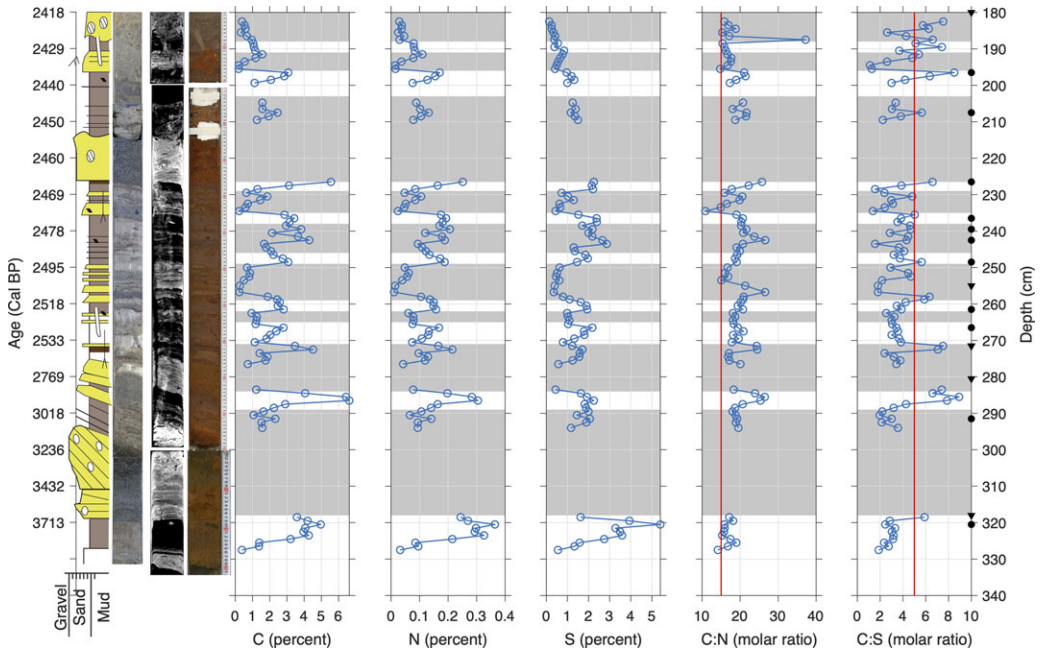

Figure 4 Results of event deposit identification. From left to right, the columnar section (Shishikura et al. 2013), core photograph taken on site, CT image, core photograph scanned with core image scanner and CNS element analysis result. The gray zones in the EA result are the locations of the identified nine event layers. C/N > 15 and C/S > 5 indicates terrestrial organic matter and freshwater, respectively. Locations of radiocarbon dates are shown on right vertical axis. Triangles are plant fragment dates, and circles are bulk organic matter dates.

1.8 m to the start of the reclaimed landfill at 1.2 m. The well-rounded sand is consistent with beach sand and thus likely transported by water flow from the sea. Without additional evidence for concurrent uplift, it is difficult to determine the origin of the overwash with only the information obtained in this study. If these sands were brought in from seaward, then strong currents may have surged over the barrier that had closed the remnants of the Paleo-Isumi Bay.

The age model also indicates that the bulk ages are typically older than the plant fragments by 400–600 years (Figure 2). While this value is similar to the global marine reservoir age in the most recent calibration curve (Marine20, Heaton et al. 2020), C/N ratios are inconsistent with a marine origin. Rather, the offset is more likely due to the inclusion of older organic matter derived from landward sources based on interpretation.

CONCLUSIONS

We conducted the description of core ISL-6 drilled in a former lagoon on the Isumi River lowland and radiocarbon dating for constructing of an age-depth model with the latest calibration curve and appropriate model routine. We identified nine sand layers and revealed that some of which were deposited by overwash between 2.4 and 2.5 cal. ky BP. These events appear associated with changes in redox condition in the lagoon which over time became increasingly isolated from the ocean due to either local seismic uplift, relative sea-level fall, enhanced barrier development, or a combination of each. At this point, the mechanism causing washover events is not yet constrained.

https://doi.org/10.1017/RDC.2023.105 Published online by Cambridge University Press

Table 3 Radiocarbon ages obtained from marine terraces uplifted during the 1923 Taisho and 1703 Genroku Earthquakes that are used to calculate local reservoir correction using the Marine20 calibration curve.

Calendar year	Cal BP 1950	Marine20 ^{14}C age	Marine20 ^{14}C age error	Shell ^{14}C age	Shell ^{14}C age error	ΔR	ΔR error
1923	27	604	63	490	40	−114	75
1923	27	604	63	560	40	−44	75
1923	27	604	63	510	40	−94	75
1923	27	604	63	580	50	−24	80
					Taisho mean:	−69	76
1703	247	760	70	620	40	−140	81
1703	247	760	70	610	40	−150	81
1703	247	760	70	670	40	−90	81
1703	247	760	70	690	40	−70	81
					Genroku mean:	−113	81
					Mean:	−91	111

ACKNOWLEDGMENTS

This research was supported by the Cooperative Program (No. 102, 2022) of Atmosphere and Ocean Research Institute, The University of Tokyo. The core sample collection and dating were partially funded by a grant from the Ministry of Education, Culture, Sports, Science, and Technology and reported in the 2012 report on investigation of Tohoku earthquakes and tsunamis generated in the offshore Pacific [東北地方太平洋沖で発生する地震・津波 の調査観測平成24年度、成果報告書] available online at: https://www.jishin.go.jp/database/project_report/tohoku_tsunami/tohoku_tsunami-h24/. Data in this study is available on the zenodo database at https://zenodo.org/doi/10.5281/zenodo.10124615.

REFERENCES

Berner RA, Raiswell R. 1984. C/S method for distinguishing freshwater from marine sedimentary rocks. Geology (12):365–368.

Biggs RB, Sharp JH, Church TM, Tramontano JM. 1983. Optical properties, suspended sediments, and chemistry associated with the turbidity maxima of the Delaware Estuary. Can. J. Fish. Aquat. Science (40):172–179.

Heaton TJ, Köhler P, Butzin M, Bard E, Reimer RW, Austin WEN, Ramsey CB, Grootes PM, Hughen KA, Kromer B, Reimer PJ, Adkins J, Burke A, Cook MS, Olsen J, Skinner LC. 2020. Marine20—the Marine Radiocarbon Age Calibration Curve (0–55,000 cal. BP). Radiocarbon 62:779–820.

Lougheed BC, Obrochta SP. 2016. MatCal: Open Source Bayesian ^{14}C Age Calibration in MATLAB. Journal of Open Research Software (4):e42.

Lougheed BC, Obrochta SP. 2019. A rapid, deterministic age-depth modeling routine for geological sequences with inherent depth uncertainty. Paleoceanography and Paleoclimatology 34:122–133.

Nagasawa R. 1979. Geomorphic development of the lower Isumi River Plain on the Boso Peninsula, central Japan. Ritsumeikan Bungaku: 412–414, 992–1014.

Nara-Watanabe, F, Watanabe, T, Lougheed, BC, and Obrochta, SP. 2023. Alternative radiocarbon age-depth model from Lake Baikal sediment: implication for past hydrological changes for last glacial to the Holocene. Radiocarbon 1–18. doi: 10.1017/RDC.2023.63

Obrochta SP, Yokoyama Y, Yoshimoto M, Yamamoto S, Miyairi Y, Nagano G, Nakamura A, Tsunematsu K, Lamair L, Hubert-Ferrari A, Lougheed BC, Hokanishi A, Yasuda A, Heyvaert VMA, Batist MD, Fujiwara O, the QuakeRecMankai Team. 2018. Mt. Fuji Holocene eruption history reconstructed from proximal lake sediments and high-density radiocarbon dating. Quaternary Science Reviews 200:395–405.

Orem WH, Burnett WC, Landing WM, Lyons WB, Showers W. 1991. Jellyfish Lake, Palau: early diagenesis of organic matter in sediments of an anoxic marine lake. Limnology and Oceanography 36(3):526–543.

Reimer PJ, Austin WEN, Bard E, Bayliss A, Blackwell PG, Ramsey CB, Butzin M, Cheng H, Edwards RL, Friedrich M, et al. 2020. The IntCal20 Northern Hemisphere radiocarbon age calibration curve (0–55 cal kBP). Radiocarbon 62(4):725–757. doi: 10.1017/RDC.2020.41

Sampei Y, Matsumoto E, Kamei T, Tokuoka T. 1997. Sulfur and organic carbon relationship in sediments from coastal brakish lakes in the Shimane peninsula district, southwest Japan. Geochemical Journal 31: 245–262.

Sakai T, Fujiwara O, Kamataki T. 2006. Incised-valley-fill succession affected by rapid tectonic uplifts: An example from the uppermost Pleistocene to Holocene of the Isumi River lowland, central Boso Peninsula, Japan. Sedimentary Geology 185:21–39.

Shishikura. M., Echigo. T., Kaneda. H. 2007. Marine reservoir correction for the Pacific coast of central Japan using ^{14}C ages of marine mollusks uplifted during historical earthquakes, Quaternary Research 67:286–291.

Shishikura M, Fujiwara O, Sawai Y, Namegaya Y, Tanikawa K, Tamura R. 2013. Research on earthquake and tsunami occurrence history based on coastal geological survey. Survey and observation on earthquake and tsunami occurrence the Pacific coast of the Tohoku Region. Earthquake Research Institute. p. 140–150.

Utsunomiya M, Oi M. 2019. Geology of the *Joso ohara* area (上総大原地域の地質) With Geological Sheet Map at 1: 50,000. Geological Survey of Japan.

Yokoyama Y, Miyairi Y, Aze T, Sawada C, Ando Y, Izawa S, Ueno Y, Hirabayashi S, Fukuyo N, Ota K, et al. 2022. Efficient radiocarbon measurements on marine and terrestrial samples with single stage Accelerator Mass Spectrometry at the Atmosphere and Ocean Research Institute, University of Tokyo. Nuclear Instruments and Methods in Physics Research Section B: Beam Interactions with Materials and Atoms 532:62–67.